

## **$J/\psi$ Longitudinal Double Spin Asymmetry Measurement at Forward Rapidity in $p + p$ Collisions at $\sqrt{s} = 510$ GeV**

Haiwang Yu

(for PHENIX Collaboration)

*School of Physics, Peking University*

*Beijing 100871, China*

*Department of Physics, New Mexico State University*

*Las Cruces NM 88003, US*

*P-25 Group, Bldg. 1, TA53, Los Alamos National Lab.*

*Los Alamos, NM 87544, US*

*yuhw@pku.edu.cn*

Published 29 February 2016

The polarized gluon distribution, as described by the polarized parton distribution function  $\Delta g(x)$ , is an important part of the spin structure of the nucleon; however the current data have very limited constraints on  $\Delta g(x)$  for  $x < 0.01$ . During the 2013 RHIC run, the PHENIX experiment collected  $146 \text{ pb}^{-1}$  of longitudinally polarized  $p + p$  data at  $\sqrt{s} = 510$  GeV with an average beam polarization of 52%. At this energy,  $J/\psi$  particles are predominantly produced through gluon-gluon interactions and thus the longitudinal double spin asymmetry,  $A_{LL}^{J/\psi}$ , is sensitive to the gluon polarization inside the proton. We measure the  $J/\psi$   $A_{LL}$  in the rapidity range  $1.2 < |\eta| < 2.4$  by detecting the decay  $\mu^+ \mu^-$  pairs using the PHENIX muon detector arms. In this kinematic range,  $A_{LL}$  is sensitive to the polarized gluon distribution at small  $x \sim 2 \times 10^{-3}$  as well as at moderate  $x \sim 0.05$  where recent RHIC data on jet and  $\pi^0$  production show possible evidence for significant gluon polarization. Compared to previous measurements in 2005 and 2006, the Run 2013 data set has roughly twenty times more statistics and will allow us to measure  $A_{LL}^{J/\psi}$  with a statistical uncertainty at  $\sim 1\%$  level. In these proceedings, the latest status of this analysis will be presented.

*Keywords:*  $A_{LL}^{J/\psi}$ ; small- $x$ ; gluon polarization.

*PACS numbers:* 14.20.Dh, 14.40.Pq

### **1. Introduction**

Gluon polarization plays an important role in understanding the proton spin structure. Including jet and  $\pi^0$  mid-rapidity data from RHIC 2009 run, the latest 2014 DSSV global fitting<sup>1</sup> shows evidence for non-zero gluon polarization. However, with

This is an Open Access article published by World Scientific Publishing Company. It is distributed under the terms of the Creative Commons Attribution 3.0 (CC-BY) License. Further distribution of this work is permitted, provided the original work is properly cited.

the mid-rapidity data alone, the gluon polarization is still poorly constrained for  $x < 0.01$ . The PHENIX experiment at RHIC is designed to be able to measure charmonia production through the di-electron channel at midrapidity and di-muon channel at forward rapidity.<sup>2</sup> PYTHIA simulation indicates measurements at forward rapidity could give us access to lower  $x$  range ( $\sim 10^{-3}$ ) at  $\sqrt{s} = 510$  GeV. In these proceedings, we present the preliminary result of longitudinal double spin asymmetry in  $J/\psi$  production through the di-muon channel at forward rapidity in p+p collisions from RHIC 2013 run data.

## 2. Motivation

Ref. 3 has shown that at RHIC energies,  $J/\psi$  particles are predominantly produced through gluon-gluon interaction. Thus at leading order, the factorization for  $J/\psi$  production can be written as Eq. 1. So the asymmetry of  $J/\psi$  production is sensitive to gluon polarization as described by Eq. 2.

$$\begin{aligned} \sigma(pp \rightarrow J/\psi X) = \\ g(x_1)g(x_2) \otimes \hat{\sigma}^{gg \rightarrow c\bar{c}}(\hat{s}) \otimes \mathcal{D}_{c\bar{c}}^{J/\psi} \end{aligned} \quad (1)$$

$$A_{LL} = \frac{\Delta\sigma}{\sigma} \sim \frac{\Delta g(x_1)}{g(x_1)} \frac{\Delta g(x_2)}{g(x_2)} \otimes \hat{a}_{LL}^{gg \rightarrow c\bar{c}} \quad (2)$$

In addition to  $J/\psi$  particles, excited charmonium states are also generated in RHIC p+p collisions. Previous studies in PHENIX indicate that the  $\chi_c$  and  $\psi'$  feed-down forms a sizable portion of the inclusive  $J/\psi$  production.<sup>4</sup> And due to limited resolution, the  $\psi'$  peak overlaps the  $J/\psi$  peak on the di-muon mass spectrum at forward rapidity in PHENIX. NRQCD and pQCD provide different gluon polarization dependency of the asymmetry of the inclusive  $J/\psi$  production.<sup>3</sup> Measurements of inclusive  $J/\psi$  asymmetry could also be helpful on distinguishing different theoretical shcemes.

Including RHIC 2009  $\pi^0$  and jets data in the central rapidity, the 2014 DSSV global fit suggests non zero polarization of gluons in the proton in the range  $0.05 < x < 1$ .<sup>1</sup> Yet at low x range ( $x < 0.05$ ), the uncertainties of DSSV are still poorly constrained.<sup>1</sup>

Our PYTHIA simulation indicates that at forward rapidity, the two gluons that generate  $J/\psi$  particles sit in very different Bjorken x region (Fig. 1). Thus instead of probing  $(\Delta g/g)^2$ , the  $J/\psi$  measurement at forward rapidity is sensitive to  $\frac{\Delta g(x_1)}{g(x_1)} \frac{\Delta g(x_2)}{g(x_2)}$ . Given that the high- $x$  gluon polarization is already constrained by RHIC 2009 data, the small- $x$  gluons give us sensitivity to  $\Delta g$  down to  $2 \times 10^{-3}$  (mean value of the low- $x$  gluon  $x$  distribution).

## 3. PHENIX Detector

The PHENIX detector consists of 2 mid-rapidity and 2 forward rapidity spectrometers. Fig. 2 shows the layout of the forward spectrometers or the “muon arms”.

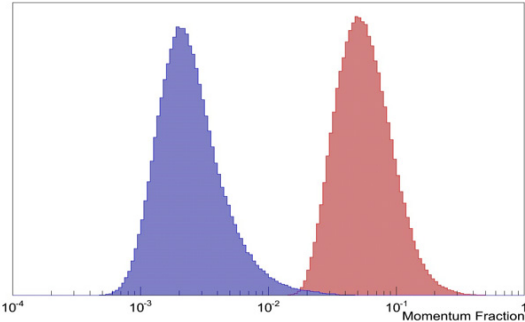


Fig. 1. (color online) Bjorken  $x$  distribution of gluons in the  $gg \rightarrow J/\psi + X \rightarrow \mu^+ \mu^- + X$  process at forward rapidity of the PHENIX detector obtained by PYTHIA simulation.

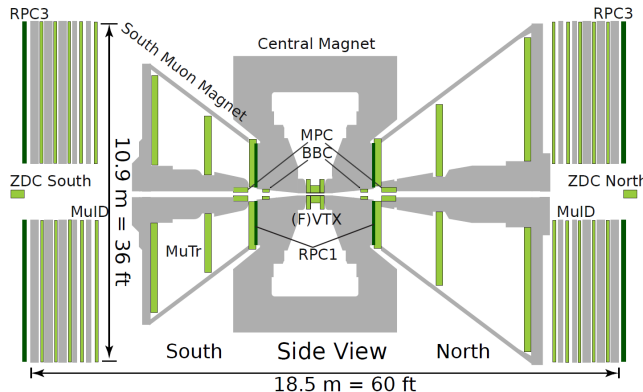


Fig. 2. (color online) Muon arm at forward rapidity of the PHENIX detector.

The muon arms have a pseudorapidity coverage of  $1.2 < |\eta| < 2.2$  and  $2\pi$  azimuthal angle coverage. Muon momentum is measured in the cathode strip tracking chambers (MuTr) and muon identification is done by the MuID which consists of 5 layers of the Iarocci tubes interleaved with steel absorbers. Two Beam Beam Counters (BBC) sit at upstream of the muon arms closer to the interaction point (IP). They measure the vertex position along the beam direction and they also serve as one of the relative luminosity detectors.

## 4. Data Analysis

### 4.1. Event and muon track selection

$J/\psi$  peak is the predominant structure of the di-muon mass spectrum at PHENIX forward rapidity making the track and event selection pretty straight forward. We

require the longitudinal ( $z$ ) position of the primary event vertex to be within 30 cm of the center of the PHENIX silicon tracker system; within this range, the muon detector efficiency is approximately constant. For muon tracks, we require (1) the muon tracker (MuTr) and muon identifier (MuID) tracking systems to agree, (2) the muons to have penetrated to at least the 4th layer of MuID steel panels, (3) both tracks to be in the same muon arm (north or south), and (4) the tracks be in the proper 100-ns beam-beam collision time window. Fig. 3 shows the di-muon invariant mass spectrum after these basic quality cuts.

#### 4.2. Asymmetry calculation

One of the advantages of the PHENIX detector is that the data from two muon arms can be analyzed separately and serve as cross-check for each other. To reveal possible  $p_T$  dependence of the asymmetry, for each arm, the data is divided into three  $p_T$  bins,  $0 \sim 2$  GeV,  $2 \sim 4$  GeV,  $4 \sim 10$  GeV. Thus, the total di-muon data is divided into 6 subsets, 3  $p_T$  bins for both arms. For each subset a fitting is done to extract the background fraction and the parameters of resonances. In the fitting, the  $J/\psi$  peak is described as a Crystal Ball function,<sup>5</sup> and the  $\psi(2S)$  peak as a Gaussian. The continuum background shape is extracted using the Gaussian Process Regression (GPR) method<sup>678</sup> with the lower and higher side-bands ( $1.5 \sim 2.2$  GeV,  $4.3 \sim 6.0$  GeV) as the training zone.

Then the di-muon spectrum of each subset is divided into 2 regions, the inclusive signal region is defined from  $\mu_{J/\psi} - 2\sigma_{J/\psi}$  to  $\mu_{J/\psi} + 2\sigma_{J/\psi}$  and the side-band region is defined from 1.5 GeV to 2.5 GeV for all the subsets. Eq. 3 is used to calculate di-muon production asymmetry for both inclusive signal region and the side-band

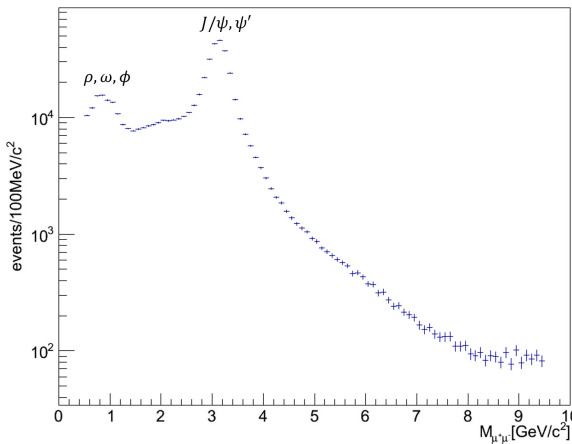


Fig. 3.  $\mu^+ \mu^-$  invariant mass spectrum base on PHENIX 2013  $p + p$  data

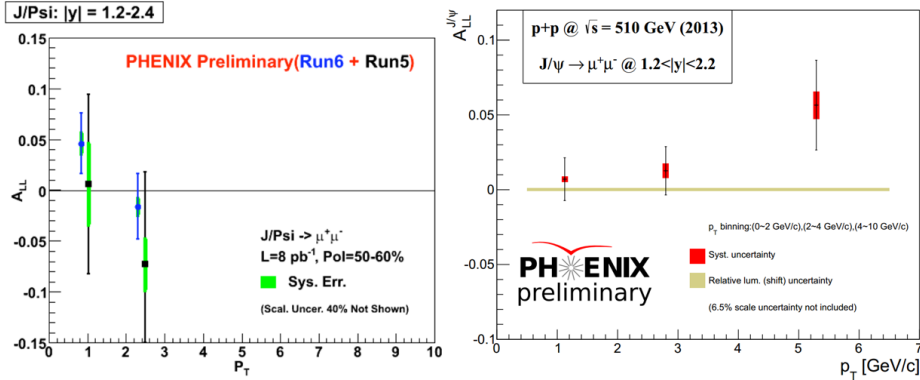


Fig. 4. (color online)  $A_{LL}^{J/\psi}$  results. Left is based on 2005, 2006 PHENIX data. Right is based on 2013 PHENIX data.

region, denoted as  $A_{LL}^{incl.}$  and  $A_{LL}^{bkg.}$  respectively. In Eq. 3, relative luminosity  $L^{++}$ ,  $L^{+-}$  are relative luminosity for like-sign helicity bunches and unlike-sign helicity bunches respectively. In this analysis, they are measured by the BBC. The  $J/\psi$  asymmetry and the statistical uncertainty for this asymmetry are extracted by Eq. 4 and 5.

### 4.3. Results

After combining results from two arms, Fig. 4 shows the  $J/\psi$   $A_{LL}$  results based on PHENIX data from 2005, 2006, and 2013 RHIC runs.

$$A_{LL} = \frac{\sigma^{++} - \sigma^{++}}{\sigma^{++} + \sigma^{++}} = \frac{1}{P_B P_Y} \frac{N^{++} - R \cdot N^{+-}}{N^{++} + R \cdot N^{+-}}, (R = \frac{L^{++}}{L^{+-}}) \quad (3)$$

$$A_{LL}^{J/\psi} = \frac{A_{LL}^{incl.} - r \cdot A_{LL}^{bkg.}}{1 - r} \quad (4)$$

$$\Delta A_{LL}^{J/\psi} = \frac{\sqrt{(\Delta A_{LL}^{incl.})^2 + r^2 \cdot (\Delta A_{LL}^{bkg.})^2}}{1 - r} \quad (5)$$

## 5. Conclusions and Outlook

The  $J/\psi$   $A_{LL}$  measurements at forward rapidity provide access to the small-x region ( $\sim 10^{-3}$ ) where the gluon polarization is poorly constrained. With the large statistics longitudinal p+p data collected at RHIC in 2013, we measured  $A_{LL}^{J/\psi}$  at forward rapidity with smaller uncertainty compared with similar prior RHIC measurements. We encourage theory community to incorporate this data in future NLO fits.

## References

1. D. de Florian, R. Sassot, M. Stratmann and W. Vogelsang, *Phys. Rev. Lett.* **113**, p. 012001 (2014), <http://arxiv.org/abs/1404.4293>.
2. K. Adcox *et al.*, *Nucl.Instrum.Meth. A* **499**, 469 (2003).
3. S. Gupta and P. Mathews, *Phys.Rev. D* **56**, 7341 (1997), <http://arxiv.org/abs/hep-ph/9706541>.
4. A. Adare *et al.*, *Phys. Rev. D* **85**, p. 092004 (2012).
5. T. Skwarnicki DESY-F31-86-02.
6. D. J. MacKay, *Information Theory, Inference and Learning Algorithms* (Cambridge University Press, 2003).
7. C. E. Rasmussen and C. K. I. Williams, *Gaussian Processes for Machine Learning* (MIT Press, 2006).
8. S. L. Lauritzen, *Graphical models* (Clarendon Press Oxford University Press, 1996).